Published as: *Nature*. ; 484(7393): 260–264.

Telomerase RNA biogenesis involves sequential binding by Sm and Lsm complexes

Wen Tang[1,2,3], **Ram Kannan**[1,2,3], **Marco Blanchette**[2,4], and **Peter Baumann**[1,2,3,*]

[1]Howard Hughes Medical Institute, University of Kansas Medical Center

[2]Stowers Institute for Medical Research, University of Kansas Medical Center

[3]Department of Molecular and Integrative Physiology, University of Kansas Medical Center

[4]Department of Pathology and Laboratory Medicine, University of Kansas Medical Center

Abstract

In most eukaryotes, the progressive loss of chromosome-terminal DNA sequences is counteracted by the enzyme telomerase, a reverse transcriptase that uses part of an RNA subunit as template to synthesize telomeric repeats. Many cancer cells express high telomerase activity and mutations in telomerase subunits are associated with degenerative syndromes including dyskeratosis congenita and aplastic anaemia. The therapeutic value of altering telomerase activity thus provides ample impetus to study the biogenesis and regulation of this enzyme in human cells and model systems. We have previously identified a precursor of the fission yeast telomerase RNA subunit (TER1)[1] and have demonstrated that the mature 3′ end is generated by the spliceosome in a single cleavage reaction akin to the first step of splicing[2]. Directly upstream and partially overlapping with the spliceosomal cleavage site is a putative Sm protein binding site. Sm and Like-Sm (LSm) proteins belong to an ancient family of RNA binding proteins represented in all three domains of life[3]. Members of this family form ring complexes on specific sets of target RNAs and play critical roles in their biogenesis, function and turnover. We now demonstrate that the canonical Sm ring and the Lsm2-8 complex sequentially associate with fission yeast TER1. The Sm ring binds to the TER1 precursor, stimulates spliceosomal cleavage and promotes the hypermethylation of the 5′ cap by Tgs1. Sm proteins are then replaced by the Lsm2-8 complex, which promotes the association with the catalytic subunit and protects the mature 3′ end of TER1 from exonucleolytic degradation. Our findings define the sequence of events that occur during telomerase biogenesis and characterize roles for Sm and Lsm complexes as well as for the methylase Tgs1.

*Correspondence: peb@stowers.org, Mailing Address: Howard Hughes Medical Institute and Stowers Institute for Medical Research, 1000 East 50th Street, Kansas City, MO 64110, U.S.A. Phone: (816) 926-4445, Fax: (816) 926-2096.

Author Contributions

P.B. and W.T. conceived the study and designed the experiments; W.T. performed most of the experiments with some assistance from those acknowledged and P.B.; R.K. contributed to the characterization of Sm mutants and analysed telomere length of myc-tagged strains. M.B. wrote the script for sequence data analysis and provided advice; W.T., R.K. and P.B. analysed the data and W.T. and P.B. wrote the manuscript.

The authors declare no competing financial interests.

In eukaryotes, seven Sm proteins (SmB, SmD1, 2 and 3, SmE, SmF, and SmG) form a heteroheptameric complex at U-rich Sm binding sites ($AU_{4–6}GR$) of various small nuclear RNAs (snRNAs) including the spliceosomal snRNAs U1, U2, U4 and U5[4,5]. Assembly of Sm proteins *in vivo* requires the help of SMN (Survival of Motor Neurons), mutations in which result in spinal muscular atrophy[6]. At least two Sm-like complexes have been characterized. The Lsm1-7 complex functions in mRNA degradation[7,8] and the Lsm2-8 complex is involved in the maturation of various polymerase III transcripts[9–11] and ribosomal RNAs[12]. Purified Lsm2-8 binds to the 3′ terminal U-tract on U6, but not to the internal U-rich Sm sites in U1, U2, U4 and U5 snRNAs, illustrating that Sm and Lsm complexes have different sets of target RNAs[9].

Sm binding sites are also found near the 3′ ends of telomerase RNA subunits from diverse yeasts[1,13–16] and are important for RNA processing and/or stability[1,2,15]. Actual binding of Sm proteins has been demonstrated for TLC1, the telomerase RNA from *S. cerevisiae*[15], but the functional consequences of this interaction have remained largely unexplored. The Sm binding site in TLC1 is located several nucleotides upstream of the mature 3′ end[13]. In contrast, spliceosomal cleavage of *S. pombe* TER1 truncates the putative Sm binding site by one nucleotide[2] which may compromise stable association of the Sm ring with mature TER1. We therefore set out to examine which proteins bind to the 3′ end of mature TER1, and to determine the function of the putative Sm site for TER1 biogenesis and stability.

A strategy was developed to examine the 3′ end of TER1 by massively parallel sequencing to obtain a quantitative measure of 3′ end sequence distribution and to identify the most abundant terminal sequences (Fig. 1a). This analysis revealed that following spliceosomal cleavage over 60% of TER1 molecules have lost additional nucleotides at the 3′ end and terminate in a stretch of 3 to 6 uridines (Fig. 1b). The 3′ end of the majority of TER1 therefore resembles the 3′ end of U6 snRNA, which is bound by the Lsm2-8 complex. To test whether Sm or Lsm proteins associate with TER1, carboxyl-terminal c-Myc epitope tags were inserted at the genomic loci of all Sm and Lsm proteins.

Immunoprecipitations were performed with a subset of strains that did not show overt growth defects, expressed tagged proteins and maintained telomeres (Suppl. Fig. 1). The snRNA U1 control specifically co-precipitated with Sm proteins confirming that the epitope tags did not interfere with immunoprecipitation of RNP complexes (Fig. 1c). TER1 co-immunoprecipitated with all four Sm proteins tested (Fig. 1c, lanes 2–4 and Suppl. Fig. 2a), including members of each of the three Sm subcomplexes[4]. Strikingly though, several-fold more TER1 was recovered from Lsm IPs resulting in an ~80% depletion of TER1 from the IP supernatant (Fig. 1c, lanes 5–7). TER1 precipitated with all subunits of the Lsm2-8 complex (Fig. 1c and Suppl. Fig. 2b), but not with Lsm1 (Fig. 1c, lane 8), the subunit specific to the Lsm1-7 complex.

To determine whether Sm and/or Lsm are associated with active telomerase, direct *in vitro* activity assays were performed on immunoprecipitates. Telomerase activity was detected in all samples, but was 20-fold higher in Lsm3 and 4 compared to Smb1 and Sme1 IPs (Fig. 1d and Suppl. Fig. 2c). In part this can be explained by the lower recovery of telomerase with Sm proteins as judged by quantification of telomerase RNA on northern blots (Suppl. Fig.

2c, d). However, even after normalization to the amount of TER1 in each IP, Lsm-associated telomerase activity was still 2.8-fold higher than the activity associated with Sm proteins. The simplest explanation for this observation is that a fraction of Sm-associated TER1 is not yet associated with the catalytic subunit of telomerase. Indeed, further experiments confirmed that Sm binding precedes Trt1 binding to TER1.

To gain insights into the functions of Sm and Lsm binding to telomerase we initially focused on the Sm association. For most characterized snRNAs, sequences downstream of the Sm binding site are critical for Sm loading[17]. As the mature form of TER1 lacks such sequences, we tested whether the Sm complex was loaded onto the TER1 precursor prior to spliceosomal cleavage. RT-PCR confirmed that the precursor is indeed specifically associated with the Sm complex, but is undetectable in Lsm immunoprecipitates (Fig. 2a).

As the spliceosome contains Sm complexes, the TER1-Sm interaction may reflect binding of the spliceosome to the TER1 precursor. To test whether Sm proteins bind TER1 directly, we generated constructs with either a mutant 5′ splice site or a deletion of the intron. Both mutant RNAs co-immunoprecipitated with Smb1 (Fig. 2b). In contrast, replacing the Sm binding sequence with a random sequence (*ter1-sm6* mutant) reduced Sm association by 22-fold (Fig. 2c). Similarly, Lsm association was undetectable for ter1-sm6 (Suppl. Fig. 3a). We therefore surmised that Sm and Lsm proteins directly bind to the previously identified site in TER1.

We next examined the effect of Sm binding on 3′ end processing by the spliceosome. Loss of Sm binding in the *ter1-sm6* mutant resulted in a 7-fold reduction in the processed form (Fig. 2d). Furthermore, a series of deletion mutants within the Sm site caused progressive inhibition of TER1 cleavage (Suppl. Fig. 3b), but not TER1 splicing (Suppl. Fig. 3c). Finally, introducing an eight-nucleotide spacer between the Sm site and 5′ cleavage site also impaired processing (Fig. 2e). In summary, weakening or abolishing Sm association with the TER1 precursor reduces spliceosomal cleavage, indicating that Sm proteins promote 3′ end processing of TER1.

A conserved feature among yeast and mammalian telomerase RNAs is the post-transcriptional hypermethylation of the 5′ cap into a 2,2,7-trimethyl guanosine (TMG) form[1,15,18]. Sm proteins were first implicated in promoting cap hypermethylation on U2 snRNA in *Xenopus* extract[19]. It was later shown *in vitro* that TMG-capping of human U1 requires the presence of SmB/B′-SmD3[4,20]. A screen for physical association with Sm proteins led to the identification of Tgs1 in budding yeast[21]. To elucidate the roles of Sm and/or Lsm in the hypermethylation of the 5′ cap on TER1, we tested which, if any, of these proteins interact with *S. pombe* Tgs1[22] by two-hybrid. Smd proteins scored positive, with Smd2 displaying the strongest interaction, and the other Sm proteins and all Lsm proteins showing weak or no interaction (Suppl. Fig. 4a). We next examined whether preventing Sm binding to TER1 affects cap hypermethylation. Whereas wild type TER1 was readily precipitated with a monoclonal antibody against the TMG cap, ter1-sm6 recovery was at least 25-fold reduced (Fig. 3a and Suppl. Fig. 4b). Only the cleaved form of TER1 was recovered in TMG IPs from wild type cells, suggesting that spliceosomal cleavage precedes

hypermethylation (Suppl. Fig. 4c). TER1 was not TMG-capped in a *tgs1*Δ strain confirming that Tgs1 is the enzyme responsible for TER1 cap hypermethylation (Suppl. Fig. 4d).

In light of the reported increase in telomerase RNA in *tgs1*Δ budding yeast [23], we were surprised to observe a 5-fold reduction in TER1 RNA in *tgs1*Δ compared to wild type in *S. pombe* (Fig. 3b). In addition, an increase in the precursor indicated a 3′ end processing defect. The viability of *tgs1*Δ cells ruled out a major splicing defect, but we consistently noted a small reduction in spliceosomal snRNAs isolated from *tgs1*Δ cells (Fig. 3b and data not shown). To differentiate between a processing defect and a direct effect of the TMG cap on TER1 stability, we mutated the spliceosomal cleavage site and inserted a hammerhead ribozyme sequence to generate the mutant ter1-5′ssmut-HH (Suppl. Fig. 4e). In this construct, processing of TER1 occurs independent of the spliceosome by ribozyme cleavage. When comparing ter1-5′ssmut-HH levels between wild type and *tgs1*Δ cells, a 2-fold reduction was observed (Fig. 3b). Taken together, these results show that *tgs1*Δ affects TER1 processing by the spliceosome as well as TER1 stability. Consistent with the exquisite dosage sensitivity for telomerase RNA in diverse species[24,25], this reduction in TER1 resulted in shorter telomeres (Fig. 3c). Neither telomerase activity nor Lsm association was reduced beyond the effects expected from the reduced steady-state level of TER1 (Suppl. Fig. 4f, g).

The majority of TER1 post spliceosomal cleavage was bound by Lsm2-8, but a small fraction was associated with Sm proteins (Fig. 1c). To investigate whether this was indicative of a switch from Sm to Lsm binding, we examined the distribution of 3′ ends in each IP by massively parallel sequencing. Around 70% of Sm-bound TER1 post-cleavage terminated precisely at the spliceosomal cleavage site (Fig. 4a and Suppl. Fig. 5a). Enrichment of this form in the Sm-bound fraction is consistent with Sm proteins binding the TER1 precursor and remaining associated with TER1 until after cleavage and cap hypermethylation have occurred. In contrast, Lsm-associated TER1 predominantly terminated in $U_{3–6}$ indicating that a switch between Sm and Lsm binding occurs after spliceosomal cleavage and is associated with exonucleolytic processing (Fig. 4a and Suppl. Fig. 5b). Consistent with the majority of telomerase activity being associated with Lsm2-8, the TER1 3′ end distribution from Trt1 immunoprecipitates was indistinguishable from that of Lsm-bound TER1.

The observation that loss of Sm binding coincided with the loss of terminal nucleotides led us to speculate that Lsm2-8 may function in protecting the 3′ end of TER1 against further exonucleolytic degradation. To test this hypothesis we attempted to generate Lsm deletion strains. Whereas most Lsm proteins are essential, *lsm1*Δ and *lsm3*Δ cells were viable. Consistent with a protective function for Lsm2-8, the levels of TER1 and U6 snRNA were ~5-fold reduced in *lsm3*Δ cells (Fig. 4b). No such effect was seen when deleting *lsm1*, nor was the level of U1 snRNA reduced in *lsm3*Δ cells. The 3′ end sequence distribution for TER1 from total RNA of *lsm3*Δ cells closely resembled the Sm-bound fraction in wild type, whereas the Lsm-bound fraction was selectively lost in the mutant (Fig. 4c and Suppl. Fig. 5c). The viability of *lsm3*Δ cells further allowed us to confirm that cap hypermethylation is unaffected by the absence of Lsm consistent with Tgs1 acting on TER1 prior to Lsm binding (Suppl. Fig. 5d).

To independently verify a role for Lsm proteins in stabilizing TER1 we took advantage of the observation that Lsm binding requires a stretch of consecutive uridines[9]. In contrast, Sm binding tolerates other nucleotides in various positions of the binding motif, as exemplified by the Sm binding site in human U1 snRNA (AAUUUGUG). When the TER1 Sm site was mutated to reduce the number of consecutive uridines, the level of mature TER1 was decreased (Fig. 5a). We next precipitated Smb1, Lsm4 and Trt1 from wild type and strains containing the ter1-SmU1 mutant. As expected, the mutation had little effect on the binding of Sm proteins (Fig. 5b). In fact, when normalized for the lower level of ter1-SmU1 compared to wild type, recovery of ter1-SmU1 with Smb1 was 1.6-fold increased. In contrast, Lsm binding was diminished by more than 20-fold. Most surprisingly, the interaction between the catalytic subunit Trt1 and telomerase RNA was also compromised in the ter1-SmU1 mutant(Fig. 5b). The normalized recovery of ter1-SmU1 with Trt1 was 15-fold lower than wild type, indicating that Lsm binding facilitates Trt1 - TER1 association, possibly by inducing a conformational change in the RNA analogous to how binding of the p65 protein facilitates telomerase assembly in *Tetrahymena*[26–28]. Consistent with the poor recovery of ter1-SmU1 in Trt1 immunoprecipitations, in vitro telomerase activity was below the level of detection (Fig. 5c).

Analysis of the 3′ end sequence distribution for ter1-SmU1 from total RNA revealed that most of the mutant RNA ends at the cleavage site(Suppl. Fig. 6). This form constituted close to 90% of ter1-SmU1 in Smb1 immunoprecipitates. In contrast, Lsm4 and Trt1 IPs predominantly recovered RNA ending in –AUUU and –AUUUG (Suppl. Fig. 6). These results further support that Trt1 preferentially associates with Lsm-bound telomerase RNA. They also confirm the role of Lsm in protecting the 3′ end of TER1 from further degradation as diminished Lsm binding coincides with an overall reduction in telomerase RNA and a shift towards the form that is bound by Sm.

Taken together our observations demonstrate that distinct populations of TER1 molecules associate with the Sm and Lsm complexes and suggest a sequence of events for TER1 biogenesis (Fig. 5d). The polyadenylated TER1 precursor is bound by the Sm complex which promotes spliceosomal cleavage and subsequent 5′ cap hypermethylation by recruiting Tgs1. The Sm ring is then replaced by the Lsm2-8 complex, which protects TER1 from exonucleolytic degradation and promotes binding of the catalytic subunit.

Despite their structural similarity and related binding motifs, Sm and Lsm complexes have different modes of RNA binding and were thought to have distinct and non-overlapping sets of target RNAs. The finding that the TER1 precursor is exclusively associated with the Sm complex, whereas the majority of mature TER1 is bound by Lsm2-8 revealed that biogenesis of telomerase RNA involves both Sm and Lsm complexes. Considering the central roles that Sm and Lsm proteins play in RNA metabolism it will be important to determine whether biogenesis of other non-coding RNAs also involves Sm and Lsm2-8 bound stages. Furthermore, it is interesting to note that several Sm/Lsm proteins have been reported to co-purify with human telomerase (hTR)[29,30] raising the possibility that they also function in TMG cap formation and telomerase assembly.

Methods Summary

Myc epitope tags were integrated at the genomic loci and immunoprecipitations were performed in whole cell extracts with anti-c-Myc antibodies. The different forms of telomerase RNA were detected by northern blotting and RT-PCR. The distribution of 3′ ends was assessed at single nucleotide resolution by preparing libraries of oligo(A)-tailed telomerase RNA and massively parallel sequencing.

Methods

Yeast strains and constructs

The genotypes of all strains used in this study are listed in table S1. Strains expressing c-Myc-tagged Sm and Lsm proteins were constructed in strain PP138 as described[31]. Mutants *ter1-sm6*, *ter1-smΔG*, *ter1-smΔUG*, *ter1-smΔU_2G*, *ter1-smΔU_3G* and *ter1-5′ssmut-HH* were integrated at the *ter1* genomic locus by gene replacement. Other *ter1* mutants were generated in the context of plasmid pJW10 using the QuikChange II XL site-directed mutagenesis kit (Stratagene) and introduced into PP407, PP694 or PP695 as described[1].

Yeast two-hybrid

Yeast two-hybrid was conducted using the Matchmaker GAL4 Two Hybrid System 3 (Clontech). Briefly, *tgs1*$^+$ cDNA was cloned into the vector pGBKT7, and each full length *lsm* and *sm* cDNA was cloned into pGADT7. Plasmids were co-transformed into the yeast strain AH109 and positive transformants were selected on SD-Leu-Trp plates. Interactions were analysed by plating 3-fold serial dilutions of overnight cultures onto SD-Leu-Trp-His-Ade plates. Plates were incubated for three days at 30 °C.

Telomere length analysis and telomerase activity assay

Cells were propagated for at least 80 to 100 generations and telomere length was analysed by Southern blotting as described[32]. Telomerase activity assays were performed on sepharose beads as described[1,33] following immunoprecipitation from cell extracts of strains harbouring Myc-tagged Trt1, Sm or Lsm proteins.

Immunoprecipitation and RNA isolation

S. pombe cells were grown in YES (yeast extract supplements)[32] and 6 litres of cell suspension were harvested by centrifugation at a density of 5×10^6 cells ml^{-1}. Cells were washed in TMG(300) (10 mM Tris-HCl, pH 8.0, 1 mM magnesium chloride, 10% (v/v) glycerol, 300 mM sodium acetate), the pellet was resuspended in two packed cell volumes of TMG(300) plus supplements (5 μg ml^{-1} chymostatin, 5 μg ml^{-1} leupeptin, 1 μg ml^{-1} pepstatin, 1 mM benzamidine, 1 mM DTT, 1 mM EDTA and 0.5 mM PMSF) and the suspension was frozen in liquid nitrogen. Cells were lysed under liquid nitrogen in a 6850 cryogenic mill (SPEX CertiPrep) with eight 2 min cycles at an impactor rate of 10 per second and a 2 min cooling time between cycles. The lysed cell powder was transferred into a 50 ml tube and allowed to thaw on ice for 30 min. Cell extracts were cleared by two rounds of centrifugation at 14,000*g* for 7 min and frozen in liquid nitrogen for storage at −80 °C. The concentration of proteins in the whole cell extract was measured by Bradford

protein assay. For c-Myc immunoprecipitation, monoclonal anti-c-Myc antibody (20 μg, Sigma) was incubated with 150 μl protein A/G agarose slurry (Calbiochem) in phosphate buffered saline at room temperature for 30 min. Beads were washed three times with TMG(300) plus supplements and whole cell extract (1.2 ml) was added at a concentration of 5 mg ml^{-1} together with RNasin (40 U, Promega), Tween 20 (0.1%) and heparin (1mg ml^{-1}). For immunoprecipitation of TMG-capped RNAs anti-TMG antibody (3 μg, Calbiochem) was bound to 50 μl proteinA/G agarose slurry (Calbiochem), washed with TMG(300) and 150 μg total *S. pombe* RNA was added in 0.7 ml TMG(300). Samples were incubated on a rotator at 4 °C for 4 hours and then washed three times with TMG(300) plus supplements and 0.1% Tween 20 and once with TMG(50) (as TMG(300) but only 50 mM sodium acetate). Protease inhibitors were omitted for TMG IPs. RNA was isolated by treatment with proteinase K (2.0 mg ml^{-1} in 0.5% (w/v) SDS, 40 mM EDTA, 20 mM Tris-HCl, pH 7.5) at 50 °C for 15 min, followed by extraction with acidic phenol and ethanol precipitation. RNA was then analysed by northern blotting, RT-PCR and 3′ end sequencing.

RNA analysis

RNA isolation and northern blotting were performed as described[2] except that Biodyne Nylon Transfer Membrane (Pall Corporation) was used and samples shown in Fig. 5a were treated with RNaseH in the presence of oligo nucleotides BLoli1043 (AGGCAGAAGACTCACGTACACTGCAC), BLoli1275 and PBoli560 (GCGGAATTCT18)to obtain better separation of precursor and mature form. The TER1 probe was generated as described[2]; other RNAs were detected using 5′ ^{32}P-labelled DNA oligonucleotides as follows:

GCTGCAGAAACTCATGCCAGGTAAGT (snRNA U1),

CGCTATTGTATGGGGCCTTTAGATTCTTA (snoRNA snR101),

CTTCATCGATGCGAGAGCCAAGAGATCCGT(5.8S rRNA), and

GCAGTGTCATCCTTGTGCAGGGGCCA (snRNA U6).

Semi-quantitative RT-PCR was performed as described previously[2] with primers BLoli1275 (CGGAAACGGAATTCAGCATGT) and BLoli1020 (CAAACAATAATGAACGTCCTG) amplifying the intron-spanning region and PBoli918 (ACAACGGACGAGCTACACTC) and BLoli1006 (CATTTAAGTGCTTGTCAGATCACAACG) amplifying a region in the first exon. BLoli2051 (GACCTTAGCCAGTCCACAGTTA) and Bloli2101 (ACCTGGCATGAGTTTCTGC) were used to amplify snRNA U1. For quantitative real-time RT-PCR reverse transcription for input and immunoprecipitated RNA were performed with antisense primer Bloli2860 (TGCTCAGACCAAGTGAAAAA) and Bloli2051. Real-time PCR was performed in triplicate 12.5 μl reactions using Power SYBR Green PCR Master Mix (Applied Biosystems) according to the manufacturer's instructions. Bloli2860 and Bloli2859 (GGATCAAAGCTTTTGCTTGT) were used to amplify the first exon of TER1. Bloli2051 and Bloli2101 were used to amplify snRNA U1. The qRT-PCR results were imported into Excel and the average value and standard deviation of triplicate Ct values were calculated. Enrichment of immunoprecipitation is represented by ΔCt (Ct value (IP sample) minus Ct value (input)) relative to the untagged control samples. Error bars in the graph represent the positive and negative range of the standard error of the mean.

3′ end cloning

DNase-treated total RNA samples (2.5 μg) or immunoprecipitated and purified RNA was incubated with poly(A) polymerase (600 U, US Biologicals), RNase inhibitor (RNasin, 40 U) and ATP (0.5 mM) in 20 μl reactions at 30 °C for 30 min. The reaction volume was increased to 35.5 μl by the addition of the oligonucleotide Bloli2327 (CAAGCAGAAGACGGCATACGA$(T)_{18}$, 125 pmol) and dNTP mix (25 nmol), and reactions were incubated at 65 °C for 3 min followed by slow cooling to room temperature. The reaction volume was then adjusted to 50 μl with first strand buffer (Invitrogen), dithiothreitol (5 mM), RNasin (40 U) and Superscript III reverse transcriptase (200 U, Invitrogen), and reactions were incubated at 50 °C for 60 min. RNaseH (5 U, NEB) was added and incubation was continued at 37 °C for 20 min. Aliquots (3 μl) of this reaction were used in PCR with Taq polymerase (5 U, NEB) and primers (GTTCAGAGTTCTACAGTCCGACGATC##GCAAAATGTTAAAAGGAACG) and Bloli2330 (CAAGCAGAAGACGGCATACGA) (200 nM each, ## represents a two-nucleotide barcode used for multiplexing) under the following conditions: 3 min at 94°C followed by 10 cycles of 30 sec at 94 °C, 45 sec at 55 °C and 60 sec at 72 °C, followed by 7 min at 72 °C. PCR products were purified using the QIAquick PCR Purification Kit (Qiagen) and eluted with 46 μl elution buffer. In the second round of PCR, 23 μl of the eluted product was amplified with Bloli2329 (AATGATACGGCGACCACCGACAGGTTCAGAGTTCTACAGTCCGA) and Bloli2330 (200 nM each) under the following conditions: 3 min at 94 °C followed by 29 cycles of 30 s at 94 °C, 45 s at 55 °C and 60 s at 72 °C, followed by 7 min at 72 °C. PCR products were separated by electrophoresis on 1.5 % agarose gels, and bands of the correct size were excised and purified. The concentration of the PCR products was measured using the Agilent 2100 Bioanalyzer (Agilent Technologies) and further adjusted to 10 nM for massively parallel sequencing using Illumina sequencing technology. Reads were analysed using a custom script written in BioPerl to filter for those that contained the TER1 sequence (GCAAAAN_{10}AACG) and sort the reads into different bins based on the two-nucleotide barcodes. The nucleotide sequence between GCAAAAN_{10}AACG and the oligo(A) sequence resulting from the poly(A) polymerase treatment represents the end of TER1 and was used to determine the 3′ end sequence distribution at single nucleotide resolution. Further analysis and graphs were prepared in Excel.

Supplementary Material

Refer to Web version on PubMed Central for supplementary material.

Acknowledgments

We thank Stewart Shuman for the *tgs1*Δ strain, Jessica A. Box, Jeremy T. Bunch, Sean Hartnett and Rachel M. Helston for technical assistance, the Molecular Biology Core Facility for site-directed mutagenesis and sequencing, Diana P. Baumann and Rachel M. Helston for proofreading of the manuscript, and all members of the Baumann laboratory for discussions. This work was funded in part by the Stowers Institute for Medical Research. R.K. is supported by an award from the American Heart Association, and P.B. is an Early Career Scientist with the Howard Hughes Medical Institute.

References

1. Leonardi J, Box JA, Bunch JT, Baumann P. TER1, the RNA subunit of fission yeast telomerase. Nat Struct Mol Biol. 2008; 15:26–33. [PubMed: 18157152]
2. Box JA, Bunch JT, Tang W, Baumann P. Spliceosomal cleavage generates the 3′ end of telomerase RNA. Nature. 2008; 456:910–914. [PubMed: 19052544]
3. Wilusz CJ, Wilusz J. Eukaryotic Lsm proteins: lessons from bacteria. Nat Struct Mol Biol. 2005; 12:1031–1036. [PubMed: 16327775]
4. Raker VA, Plessel G, Luhrmann R. The snRNP core assembly pathway: identification of stable core protein heteromeric complexes and an snRNP subcore particle in vitro. EMBO J. 1996; 15:2256–2269. [PubMed: 8641291]
5. Patel SB, Bellini M. The assembly of a spliceosomal small nuclear ribonucleoprotein particle. Nucleic Acids Res. 2008; 36:6482–6493. [PubMed: 18854356]
6. Terns MP, Terns RM. Macromolecular complexes: SMN--the master assembler. Curr Biol. 2001; 11:R862–864. [PubMed: 11696342]
7. Tharun S, et al. Yeast Sm-like proteins function in mRNA decapping and decay. Nature. 2000; 404:515–518. [PubMed: 10761922]
8. Bouveret E, Rigaut G, Shevchenko A, Wilm M, Seraphin B. A Sm-like protein complex that participates in mRNA degradation. EMBO J. 2000; 19:1661–1671. [PubMed: 10747033]
9. Achsel T, et al. A doughnut-shaped heteromer of human Sm-like proteins binds to the 3′-end of U6 snRNA, thereby facilitating U4/U6 duplex formation in vitro. EMBO J. 1999; 18:5789–5802. [PubMed: 10523320]
10. Mayes AE, Verdone L, Legrain P, Beggs JD. Characterization of Sm-like proteins in yeast and their association with U6 snRNA. EMBO J. 1999; 18:4321–4331. [PubMed: 10428970]
11. Kufel J, Allmang C, Verdone L, Beggs JD, Tollervey D. Lsm proteins are required for normal processing of pre-tRNAs and their efficient association with La-homologous protein Lhp1p. Mol Cell Biol. 2002; 22:5248–5256. [PubMed: 12077351]
12. Kufel J, Allmang C, Petfalski E, Beggs J, Tollervey D. Lsm Proteins are required for normal processing and stability of ribosomal RNAs. J Biol Chem. 2003; 278:2147–2156. [PubMed: 12438310]
13. Dandjinou AT, et al. A phylogenetically based secondary structure for the yeast telomerase RNA. Curr Biol. 2004; 14:1148–1158. [PubMed: 15242611]
14. Gunisova S, et al. Identification and comparative analysis of telomerase RNAs from Candida species reveal conservation of functional elements. RNA. 2009; 15:546–559. [PubMed: 19223441]
15. Seto AG, Zaug AJ, Sobel SG, Wolin SL, Cech TR. Saccharomyces cerevisiae telomerase is an Sm small nuclear ribonucleoprotein particle. Nature. 1999; 401:177–180. [PubMed: 10490028]
16. Webb CJ, Zakian VA. Identification and characterization of the Schizosaccharomyces pombe TER1 telomerase RNA. Nat Struct Mol Biol. 2008; 15:34–42. [PubMed: 18157149]
17. Yong J, Kasim M, Bachorik JL, Wan L, Dreyfuss G. Gemin5 delivers snRNA precursors to the SMN complex for snRNP biogenesis. Mol Cell. 2010; 38:551–562. [PubMed: 20513430]
18. Jady BE, Bertrand E, Kiss T. Human telomerase RNA and box H/ACA scaRNAs share a common Cajal body-specific localization signal. J Cell Biol. 2004; 164:647–652. [PubMed: 14981093]
19. Mattaj IW. Cap trimethylation of U snRNA is cytoplasmic and dependent on U snRNP protein binding. Cell. 1986; 46:905–911. [PubMed: 2944599]
20. Plessel G, Fischer U, Luhrmann R. m3G cap hypermethylation of U1 small nuclear ribonucleoprotein (snRNP) in vitro: evidence that the U1 small nuclear RNA-(guanosine-N2)-methyltransferase is a non-snRNP cytoplasmic protein that requires a binding site on the Sm core domain. Mol Cell Biol. 1994; 14:4160–4172. [PubMed: 8196654]
21. Mouaikel J, Verheggen C, Bertrand E, Tazi J, Bordonne R. Hypermethylation of the cap structure of both yeast snRNAs and snoRNAs requires a conserved methyltransferase that is localized to the nucleolus. Mol Cell. 2002; 9:891–901. [PubMed: 11983179]

22. Hausmann S, Ramirez A, Schneider S, Schwer B, Shuman S. Biochemical and genetic analysis of RNA cap guanine-N2 methyltransferases from Giardia lamblia and Schizosaccharomyces pombe. Nucleic Acids Res. 2007; 35:1411–1420. [PubMed: 17284461]
23. Franke J, Gehlen J, Ehrenhofer-Murray AE. Hypermethylation of yeast telomerase RNA by the snRNA and snoRNA methyltransferase Tgs1. J Cell Sci. 2008; 121:3553–3560. [PubMed: 18840651]
24. Harrington L. Making the most of a little: dosage effects in eukaryotic telomere length maintenance. Chromosome Res. 2005; 13:493–504. [PubMed: 16132814]
25. Mozdy AD, Cech TR. Low abundance of telomerase in yeast: implications for telomerase haploinsufficiency. RNA. 2006; 12:1721–1737. [PubMed: 16894218]
26. Berman AJ, Gooding AR, Cech TR. Tetrahymena telomerase protein p65 induces conformational changes throughout telomerase RNA (TER) and rescues telomerase reverse transcriptase and TER assembly mutants. Mol Cell Biol. 2010; 30:4965–4976. [PubMed: 20713447]
27. O'Connor CM, Collins K. A novel RNA binding domain in tetrahymena telomerase p65 initiates hierarchical assembly of telomerase holoenzyme. Mol Cell Biol. 2006; 26:2029–2036. [PubMed: 16507983]
28. Stone MD, et al. Stepwise protein-mediated RNA folding directs assembly of telomerase ribonucleoprotein. Nature. 2007; 446:458–461. [PubMed: 17322903]
29. Fu D, Collins K. Human telomerase and Cajal body ribonucleoproteins share a unique specificity of Sm protein association. Genes Dev. 2006; 20:531–536. [PubMed: 16481465]
30. Fu D, Collins K. Purification of human telomerase complexes identifies factors involved in telomerase biogenesis and telomere length regulation. Mol Cell. 2007; 28:773–785. [PubMed: 18082603]
31. Bahler J, et al. Heterologous modules for efficient and versatile PCR-based gene targeting in Schizosaccharomyces pombe. Yeast. 1998; 14:943–951. [PubMed: 9717240]
32. Bunch JT, Bae NS, Leonardi J, Baumann P. Distinct requirements for Pot1 in limiting telomere length and maintaining chromosome stability. Mol Cell Biol. 2005; 25:5567–5578. [PubMed: 15964812]
33. Haering CH, Nakamura TM, Baumann P, Cech TR. Analysis of telomerase catalytic subunit mutants in vivo and in vitro in Schizosaccharomyces pombe. Proc Natl Acad Sci U S A. 2000; 97:6367–6372. [PubMed: 10829083]

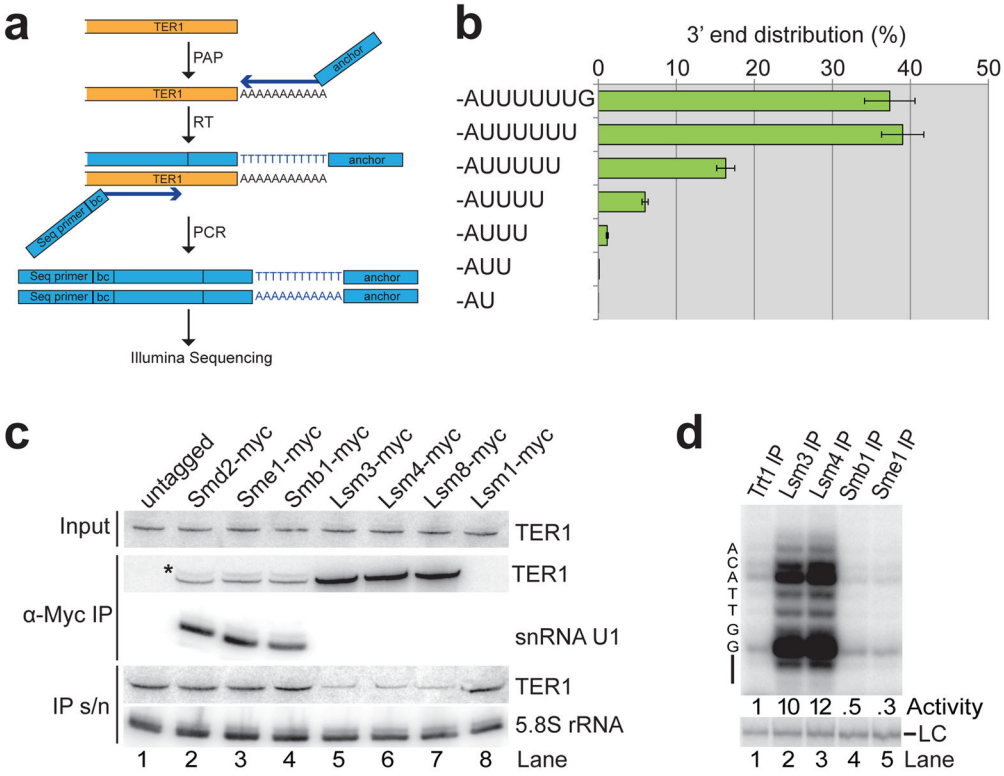

Fig. 1.

TER1 RNA associates with Sm and Lsm proteins. **(a)** Schematic of method used to map the 3′ end distribution of TER1 post spliceosomal cleavage. RNA is depicted in orange, DNA in blue. Abbreviations: PAP, poly(A) polymerase; RT, reverse transcription; PCR, polymerase chain reaction; bc, barcode. **(b)** Distribution of 3′ end positions in mature TER1 from wild type cells. The average of four experiments is shown, error bars represent standard deviation, a total of 23×10^6 sequences were scored. **(c)** Northern blot of RNA isolated from immunoprecipitations with anti-c-Myc antibodies. Input and IP supernatant (s/n) represent 10% of the sample. An asterisk marks the position of the TER1 precursor. The lower band corresponds to the mature form of TER1. **(d)** Telomerase activity assay performed on beads following c-Myc immunoprecipitation of tagged proteins as indicated above each lane. Activity was quantified relative to the Trt1 IP sample. A ^{32}P-labelled 100mer oligonucleotide was used as recovery and loading control (LC).

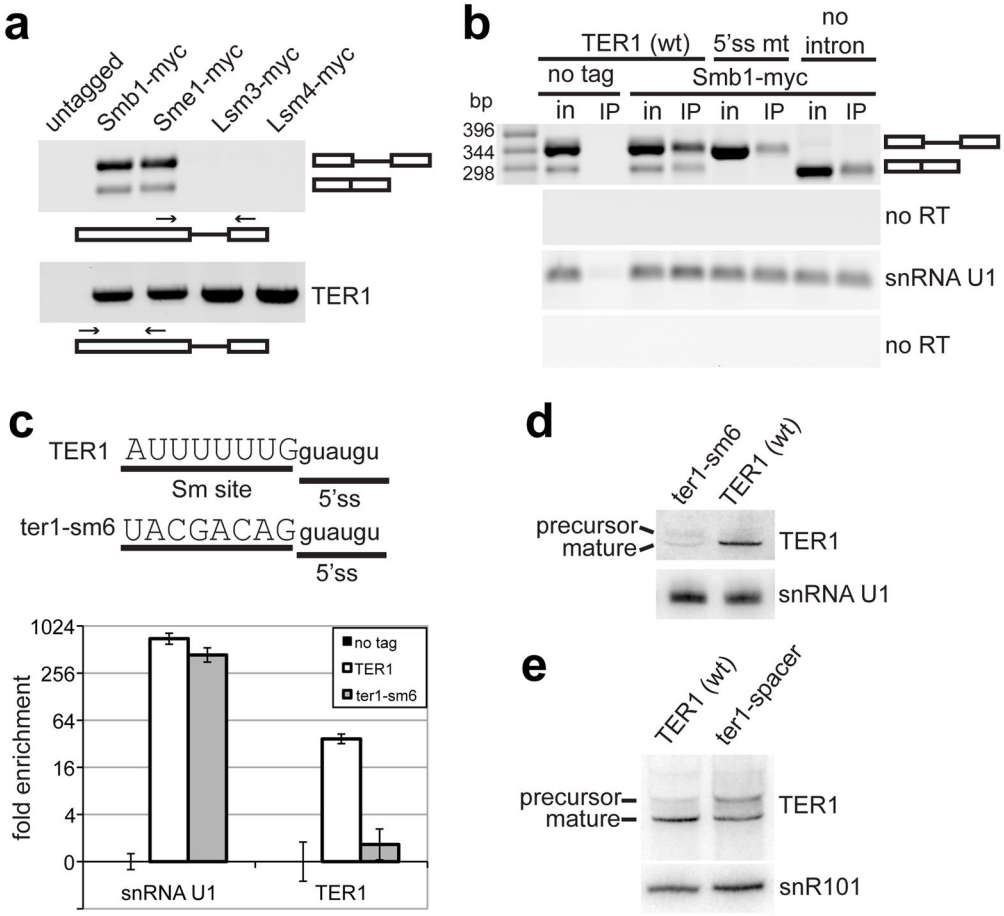

Fig. 2.

Sm proteins associate with TER1 precursor and promote spliceosomal cleavage. **(a)** RNA from α-c-Myc IPs was analysed by RT-PCR using primers in the first and second exon (primers represented by arrows in the schematic below the gel) to amplify the precursor form (upper panel). The primer pair also amplifies the spliced form (lower band in Sm IPs). A primer pair in the first exon was used to visualize all forms of TER1 combined (lower panel). **(b)** Sm association does not require spliceosome assembly on TER1. RT-PCR was performed on RNA purified from input (in) and α-c-Myc IP beads (IP). Primers that amplify snRNA U1 were used as a positive control. **(c)** Schematic of the Sm binding site (upper case) and 5′ splice site (5′ss, lower case) for wild type TER1 and the ter1-sm6 mutant. Replacing the Sm binding site on TER1 (ter1-sm6 mutant) compromises Sm association. RNA recovered from α-c-Myc IPs from untagged control and Smb1-myc strains was quantified by real time PCR. Data is plotted as enrichment over the untagged control. The error bars represent standard error of triplicate experiments. **(d)** Sm site mutation affects TER1 spliceosomal cleavage. Total RNA samples were analysed by northern blot for TER1 and snRNA U1. **(e)** Increasing the distance between the Sm site and 5′ splice site in the ter1-spacer mutant ($AU_6GgccauaugGU$) impairs TER1 processing. Northern blot for TER1 and snoRNA snR101 as loading control.

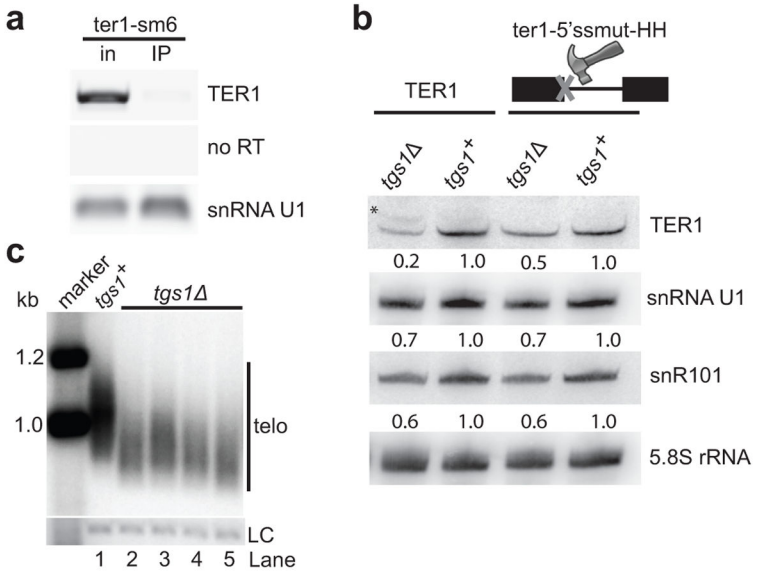

Fig. 3.

Tgs1 modifies TER1 and is required for normal telomere maintenance. **(a)** Loss of Sm site compromises TMG cap formation. RT-PCR amplifying all forms of TER1 and ter1-sm6 from α-TMG IP samples, RT=reverse transcriptase, snRNA U1 served as control. **(b)** Bypass of spliceosomal cleavage reveals functions of Tgs1 in TER1 processing and stability. Northern blot analysis of TER1, snRNA U1, snR101 and 5.8s rRNA from total RNA prepared from wild type and *tgs1*Δ strains harbouring either TER1 or the ter1-5′ssmut-HH mutant. An asterisk marks the position of the TER1 precursor. **(c)** Deletion of $tgs1^+$ causes telomere shortening. Telomere length was analysed by Southern blotting of EcoRI-digested genomic DNA from four independent *tgs1*Δ isolates and an otherwise isogenic $tgs1^+$ strain. A probe for the *rad16* gene was used as a loading control (LC).

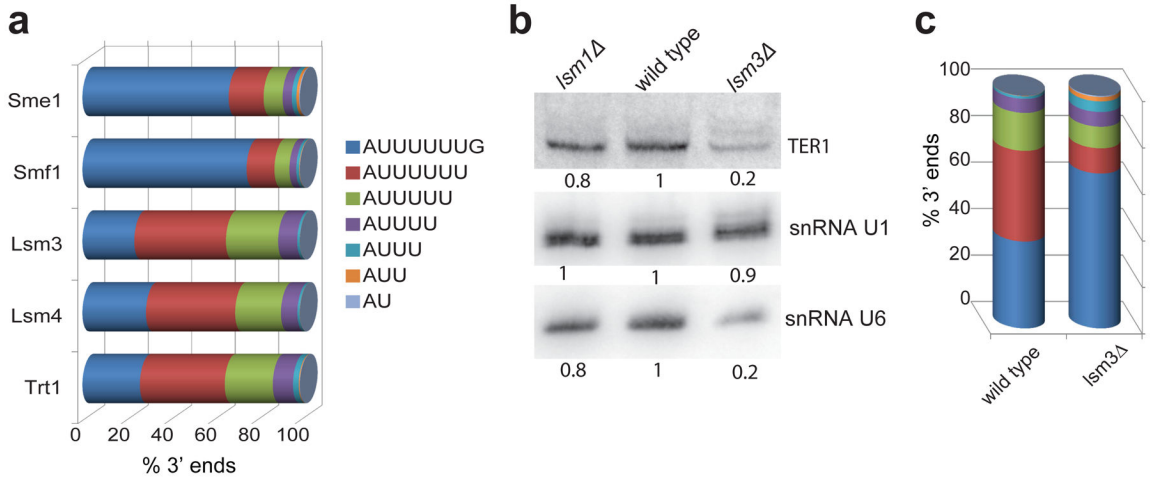

Fig. 4.

Lsm proteins replace Sm and protect the 3′ end of TER1. **(a)** 3′ end sequence distribution of TER1 from IP samples. **(b)** Northern blot analysis from total RNA prepared from wild type, *lsm1*Δ and *lsm3*Δ *strains*, quantified relative to wild type for each RNA. **(c)** Specific loss of Lsm2-8 bound fraction of TER1 in *lsm3*Δ cells based on 3′ end sequence analysis from total RNA samples. The wild type sample from Fig. 1b is included for comparison.

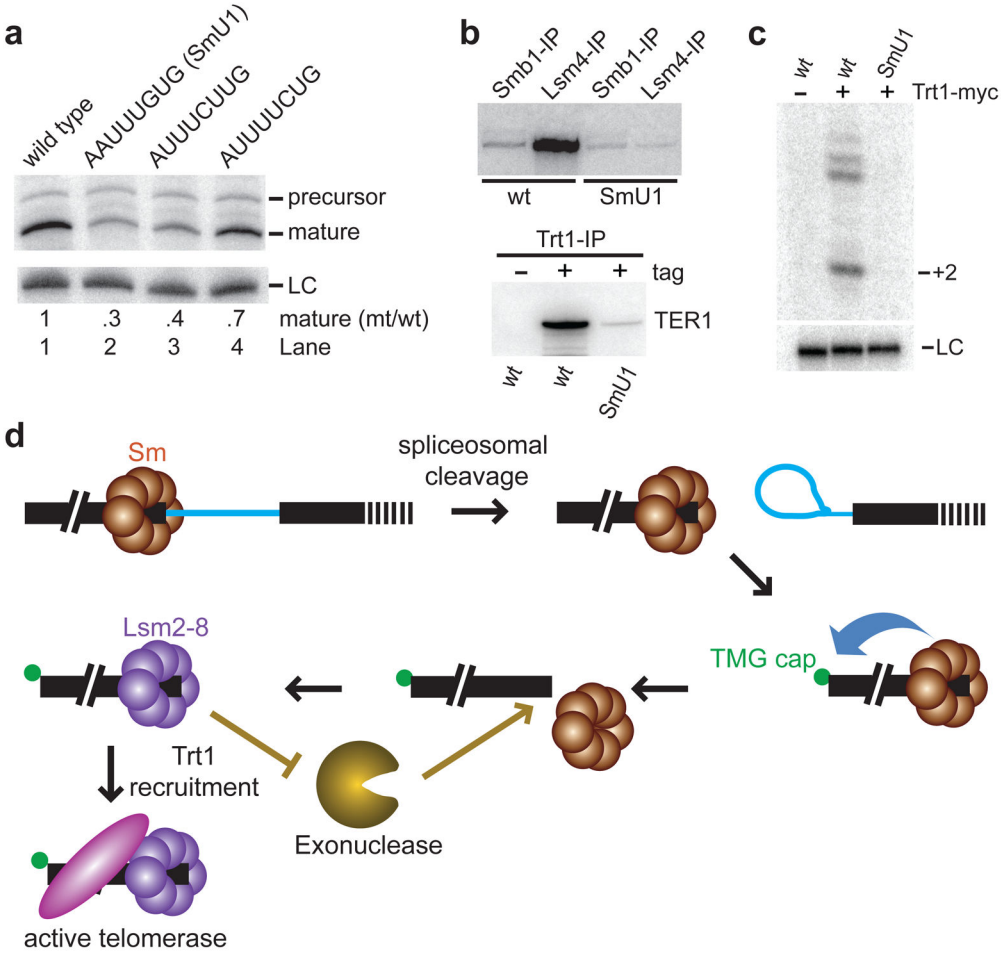

Fig. 5.

Lsm binding to TER1 promotes telomerase assembly and protects TER1 from degradation. **(a)** Northern blot for TER1. The indicated ratios of mutant to wild type are normalized to the loading control snR101 (LC). **(b)** Northern blot for TER1 and the ter1-SmU1 mutant using RNA isolated from α-c-Myc IPs performed on extract from strains harbouring Smb1-myc, Lsm4-myc or Trt1-myc as indicated. **(c)** Telomerase activity assay performed on Trt1 immunoprecipitates from strains harbouring either wild type or ter1-SmU1. An untagged Trt1 strain was used as negative control. **(d)** Schematic of the sequence of events that occur during telomerase biogenesis.